Available online at www.sciencedirect.com
SCIENCE DIRECT®
PERGAMON
International Journal of Heat and Mass Transfer 46 (2003) 4499–4512
International Journal of HEAT and MASS TRANSFER
www.elsevier.com/locate/ijhmt

Non-axisymmetric forced and free flow in a vertical circular duct

A. Barletta *, S. Lazzari, E. Zanchini

Dipartimento di Ingegneria Energetica, Nucleare e del Controllo Ambientale (DIENCA), Università di Bologna, Viale Risorgimento 2, I-40136 Bologna, Italy

Received 25 November 2002

Abstract

The fully developed laminar mixed convection in a vertical circular duct is studied analytically, with reference to non-axisymmetric boundary conditions such that the fluid temperature does not change along the axial direction. The Boussinesq approximation is applied by taking the average temperature in a duct section as the reference fluid temperature. The dimensionless momentum and energy balance equations are solved by employing Fourier series expansions of the temperature and the velocity fields. The solution shows that the temperature field is not influenced by the velocity distribution and that the Fanning friction factor is not affected by buoyancy. On the other hand, the velocity field is strongly influenced by the buoyancy forces and may display flow reversal phenomena. Two special cases are studied in detail: a duct with a sinusoidal wall temperature distribution; a duct subjected to an external convection heat transfer with two environments having different reference temperatures.

Keywords: Non-axisymmetric boundary conditions; Circular duct; Mixed convection; Laminar flow; Analytical methods

1. Introduction

The laminar mixed convection in vertical or inclined circular ducts has been studied by several authors. A wide description of the literature on this subject can be found, for instance, in [1,2]. Morton [3] presents an analytical solution of fully developed mixed convection in a vertical tube in the case of laminar flow with a uniform wall heat flux. Lawrence and Chato [4] investigate numerically the combined forced and free flow in the entrance region of a vertical tube with either a uniform wall heat flux or a uniform temperature. A numerical and experimental study of mixed convection developing flow in an isothermal vertical tube is presented by Zeldin and Schmidt [5]. They refer to upward flow and find a heat transfer enhancement for an inlet temperature higher than the wall temperature. An extension of the numerical study presented in Ref. [5] to include the case of inclined tubes can be found in Ref. [6]. Conditions for the onset of flow reversal in developing mixed convection flow of air in a vertical tube have been determined numerically by Moutsoglou and Kwon [7] for either a uniform wall heat flux or a uniform wall temperature. Buoyancy induced secondary flow in inclined tubes has been investigated numerically by Orfi et al. [8] in the special case of fully developed regime for either isothermal or uniformly heated wall. These authors show that, for given values of the Grashof number and the Prandtl number, there exists an inclination angle which maximizes the average Nusselt number and provide correlations for this quantity with different tube inclinations. In Refs. [9,10], analytical studies of the effect of viscous dissipation on mixed convection flow in a vertical circular tube are studied by employing a perturbation method.

Most papers on combined forced and free flow in vertical or inclined circular ducts refer to axisymmetric thermal boundary conditions. As is well known, there

* Corresponding author. Tel.: +390-51-644-1703; fax: +390-51-644-1747.
E-mail address: antonio.barletta@mail.ing.unibo.it (A. Barletta).

0017-9310/$ - see front matter © 2003 Elsevier Ltd. All rights reserved.
doi:10.1016/S0017-9310(03)00284-9

Nomenclature

$a_0(r)$, $a_n(r)$, $b_n(r)$ Fourier series coefficients employed in Eq. (16)
$A(\vartheta)$, $B(\vartheta)$ functions defined by Eqs. (58) and (59)
A_n, B_n integration constants employed in Eqs. (19) and (22)
Bi Biot number, defined by Eq. (78)
$c_0(r)$, $c_n(r)$, $h_n(r)$ Fourier series coefficients employed in Eq. (27)
f Fanning friction factor, defined by Eq. (45)
$F(\vartheta)$ dimensionless function defined by Eq. (75)
$\mathbf{g}$ gravitational acceleration
g magnitude of the gravitational acceleration
G arbitrary function defined on a duct section
Gr Grashof number, defined in Eq. (8)
$(Gr/Re)_{\mathrm{FR}}$ threshold value of Gr/Re for the onset of flow reversal
$(Gr/Re)_{\mathrm{sing}}$ threshold value of Gr/Re for the occurrence of singularities of Nu
h_{e} external convection coefficient
h_ϑ local convection coefficient
m, n, q non-negative integers
Nu_ϑ local Nusselt number defined by Eq. (50)
p pressure
P $= p + \varrho_0 g X$, difference between the pressure and the hydrostatic pressure
$q_{\mathrm{w}\vartheta}$ local heat flux per unit area at the wall
r dimensionless radial coordinate defined in Eq. (8)
R radial coordinate
$\mathbf{R}$ radial unit vector
R_0 radius of the channel
Re Reynolds number, defined in Eq. (8)
t dimensionless temperature, defined in Eq. (8)
t_{b} dimensionless bulk temperature, defined by Eq. (52)
T temperature
T_{b} bulk temperature of the fluid, defined by Eq. (51)
$T_f(\vartheta)$ environment temperature
T_{m} mean environment temperature
T_0 average fluid temperature, defined by Eq. (2)
T_1, T_2 reference environment temperatures
T_{w} mean wall temperature
u dimensionless velocity, defined in Eq. (8)
$u^{(1)}$, $u^{(2)}$ dimensionless functions defined by Eqs. (42) and (43)
u^* modified dimensionless velocity, defined by Eq. (44)
$\mathbf{U}$ fluid velocity
U X-component of the fluid velocity
U_0 average velocity in a channel section, defined by Eq. (9)
X axial coordinate

Greek symbols

α thermal diffusivity
β volumetric coefficient of thermal expansion
δ Kronecker's delta
ΔT reference temperature difference
η dimensionless parameter defined in Eq. (62)
ϑ angular coordinate
$\vartheta_{\mathrm{sing}}$ value of ϑ such that Nu_ϑ presents a singularity
k thermal conductivity of the fluid
λ dimensionless pressure drop, defined in Eq. (8)
μ dynamic viscosity
ν kinematic viscosity
ϱ mass density
ϱ_0 mass density for $T = T_0$
τ_{w} average wall shear stress, defined by Eq. (46)

are several technical cases such that both the wall temperature and the wall heat flux depend on the angular coordinate. Non-axisymmetric thermal boundary conditions have been studied, for instance, by Reynolds [11] and, more recently, by Choi and Choi [12,13]. Reynolds [11] obtains an analytical solution in the case of forced convection in a circular tube such that the wall heat flux undergoes a stepwise change along the angular direction, while it is kept uniform in the axial direction. Choi and Choi [12,13] present a numerical investigation of mixed convection in a horizontal tube such that the upper half of the duct wall is insulated while the lower half is subjected to a uniform heat flux.

In the present paper, the laminar mixed convection in a vertical tube is studied with reference to thermal boundary conditions such that the fluid temperature is uniform along the axial direction and is a function of the angular coordinate. The fully developed region is considered. The Boussinesq approximation is applied and the average fluid temperature in a duct section is chosen as the reference temperature. As it has been shown in Ref. [14], this choice ensures the highest accuracy of the linear relation between density and temperature. The momentum and energy balance equations, written in a dimensionless form, are solved by employing an analytical method based on Fourier series expansions of both the temperature field and the velocity field with respect to the angular coordinate. Two special cases are discussed in detail. First, a circular duct with a sinusoidal wall temperature distribution is analyzed. Then,

the case of a circular duct subjected to an external convection heat transfer with two environments having different reference temperatures is considered. This thermal boundary condition includes that of a piecewise uniform wall temperature as a limiting case, when the convection coefficient tends to infinity.

2. Mathematical model

The steady and fully developed laminar flow of a Newtonian fluid in a vertical circular duct with radius R_0 is considered. A sketch of the duct and of the cylindrical coordinate system (R,ϑ,X) is reported in Fig. 1. The flow is assumed to be parallel, so that the only non-vanishing component of the velocity vector $\mathbf{U}$ is U, along the X-direction. Moreover, the effect of viscous dissipation is neglected.

The Boussinesq approximation is employed, so that $\mathbf{U}$ is considered as a solenoidal field and, therefore, $\partial U/\partial X = 0$.

The equation of state is written in the linear form

$$\varrho = \varrho_0[1-\beta(T-T_0)], \tag{1}$$

where T_0 is the average fluid temperature on a duct cross section, namely

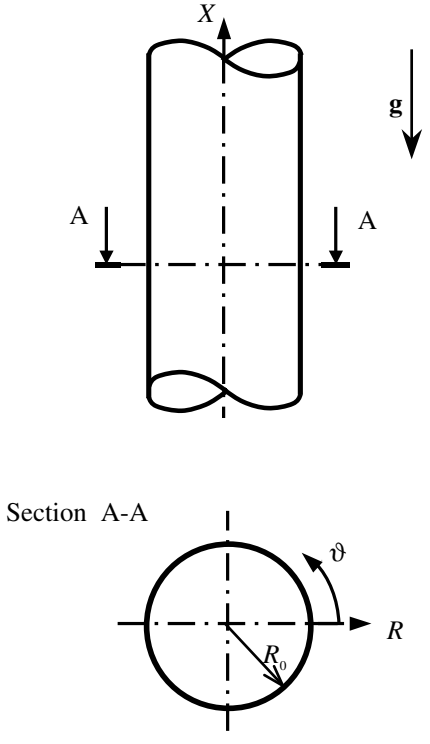

Fig. 1. Drawing of the vertical circular duct.

$$T_0 = \frac{1}{\pi R_0^2}\int_0^{2\pi} \mathrm{d}\vartheta \int_0^{R_0} \mathrm{d}R\, RT(R,\vartheta,X). \tag{2}$$

The momentum balance equations along X, R and ϑ can be written as

$$0 = -\frac{\partial P}{\partial X} + \varrho_0 g\beta(T-T_0) + \mu\left(\frac{\partial^2 U}{\partial R^2} + \frac{1}{R}\frac{\partial U}{\partial R} + \frac{1}{R^2}\frac{\partial^2 U}{\partial \vartheta^2}\right), \tag{3}$$

$$0 = -\frac{\partial P}{\partial R}, \tag{4}$$

$$0 = -\frac{1}{R}\frac{\partial P}{\partial \vartheta}, \tag{5}$$

where $P = p + \varrho_0 gX$ is the difference between the pressure and the hydrostatic pressure. The thermal boundary conditions are such that there is no net fluid heating in the axial direction, *i.e.* $\partial T/\partial X = 0$. Obviously, in this case, the reference temperature T_0 is a constant. Eqs. (4) and (5) ensure that P depends only on X.

If both sides of Eq. (3) are differentiated with respect to X, one obtains

$$\frac{\mathrm{d}^2 P}{\mathrm{d}X^2} = 0, \tag{6}$$

so that $\mathrm{d}P/\mathrm{d}X$ is a constant.

Since the effect of viscous dissipation is neglected and $\partial T/\partial X = 0$, the energy balance equation is given by

$$\frac{\partial^2 T}{\partial R^2} + \frac{1}{R}\frac{\partial T}{\partial R} + \frac{1}{R^2}\frac{\partial^2 T}{\partial \vartheta^2} = 0. \tag{7}$$

Let us define the dimensionless quantities

$$t = \frac{T-T_0}{\Delta T}, \quad u = \frac{U}{U_0}, \quad r = \frac{R}{R_0}, \quad \lambda = -\frac{4R_0^2}{\mu U_0}\frac{\mathrm{d}P}{\mathrm{d}X},$$
$$Re = \frac{2R_0 U_0}{\nu}, \quad Gr = \frac{8g\beta\Delta T R_0^3}{\nu^2}, \tag{8}$$

where U_0 is the average velocity in a duct section, namely

$$U_0 = \frac{1}{\pi R_0^2}\int_0^{2\pi} \mathrm{d}\vartheta \int_0^{R_0} \mathrm{d}R\, RU(R,\vartheta). \tag{9}$$

Obviously, U_0 is a constant. On account of Eq. (8),

$$\frac{Gr}{Re} = \frac{4g\beta\Delta T R_0^2}{\nu U_0}. \tag{10}$$

In the following, it will be assumed that ΔT is a positive quantity, so that positive values of Gr/Re imply positive values of U_0 (upward flow), while negative values of Gr/Re imply negative values of U_0 (downward flow).

Eqs. (3) and (7) can be rewritten as

$$\frac{Gr}{Re}t + \lambda + 4\left(\frac{\partial^2 u}{\partial r^2} + \frac{1}{r}\frac{\partial u}{\partial r} + \frac{1}{r^2}\frac{\partial^2 u}{\partial \vartheta^2}\right) = 0, \tag{11}$$

$$\frac{\partial^2 t}{\partial r^2}+\frac{1}{r}\frac{\partial t}{\partial r}+\frac{1}{r^2}\frac{\partial^2 t}{\partial \vartheta^2}=0. \tag{12}$$

The no slip condition at the wall implies that

$$u(1,\vartheta)=0. \tag{13}$$

In addition, both the dimensionless velocity and the dimensionless temperature on the duct axis must be finite. Finally, Eqs. (2) and (9) imply the following constraints on the functions $t(r,\vartheta)$ and $u(r,\vartheta)$:

$$\int_0^{2\pi} d\vartheta \int_0^1 dr\, rt = 0, \tag{14}$$

$$\int_0^{2\pi} d\vartheta \int_0^1 dr\, ru = \pi. \tag{15}$$

3. Analytical solution

Since the function $t(r,\vartheta)$ is continuous for $0\leqslant r<1$ and $0\leqslant\vartheta<2\pi$, it can be expanded as a Fourier series in the variable ϑ, as follows:

$$t(r,\vartheta)=\frac{a_0(r)}{2}+\sum_{n=1}^{\infty}[a_n(r)\sin(n\vartheta)+b_n(r)\cos(n\vartheta)]. \tag{16}$$

By substituting Eq. (16) in Eq. (12), one obtains

$$\frac{1}{2}\left(\frac{d^2a_0}{dr^2}+\frac{1}{r}\frac{da_0}{dr}\right)+\sum_{n=1}^{\infty}\left[\left(\frac{d^2a_n}{dr^2}+\frac{1}{r}\frac{da_n}{dr}-\frac{n^2}{r^2}a_n\right)\sin(n\vartheta)+\left(\frac{d^2b_n}{dr^2}+\frac{1}{r}\frac{db_n}{dr}-\frac{n^2}{r^2}b_n\right)\cos(n\vartheta)\right]=0. \tag{17}$$

The integration of Eq. (17) with respect to ϑ in the range $[0,2\pi]$ yields

$$\frac{d^2a_0}{dr^2}+\frac{1}{r}\frac{da_0}{dr}=0. \tag{18}$$

The general solution of Eq. (18) is

$$a_0(r)=A_0\ln r+B_0, \tag{19}$$

where A_0 and B_0 are integration constants.

Since the dimensionless temperature must be finite on the duct axis, A_0 must vanish. Moreover, on account of Eq. (14), also B_0 vanishes. Thus, Eq. (19) yields

$$a_0(r)=0. \tag{20}$$

If Eq. (17) is multiplied by $\sin(m\vartheta)$, where m is an arbitrary positive integer, and then integrated with respect to ϑ in the range $[0,2\pi]$, the following equation is obtained:

$$\frac{d^2a_n}{dr^2}+\frac{1}{r}\frac{da_n}{dr}-\frac{n^2}{r^2}a_n=0. \tag{21}$$

The general solution of Eq. (21) is

$$a_n(r)=A_nr^n+B_nr^{-n}, \tag{22}$$

where A_n and B_n are integration constants.

Since the dimensionless temperature on the duct axis must be finite, B_n must be zero and, as a consequence,

$$a_n(r)=a_n(1)r^n. \tag{23}$$

Similarly, by multiplying Eq. (17) by $\cos(m\vartheta)$ and then integrating with respect to ϑ in the range $[0,2\pi]$, one obtains

$$\frac{d^2b_n}{dr^2}+\frac{1}{r}\frac{db_n}{dr}-\frac{n^2}{r^2}b_n=0. \tag{24}$$

The general solution of Eq. (24) which is finite for $r=0$ is given by

$$b_n(r)=b_n(1)r^n. \tag{25}$$

The coefficients $a_n(1)$ and $b_n(1)$ are determined by the thermal boundary conditions. Eqs. (16), (20), (23) and (25) yield

$$t(r,\vartheta)=\sum_{n=1}^{\infty}r^n[a_n(1)\sin(n\vartheta)+b_n(1)\cos(n\vartheta)]. \tag{26}$$

The dimensionless velocity distribution can be determined by a similar procedure. In fact, the function $u(r,\vartheta)$ is continuous for $0\leqslant r<1$ and $0\leqslant\vartheta<2\pi$, so that it can be expanded as a Fourier series in the variable ϑ, as follows:

$$u(r,\vartheta)=\frac{c_0(r)}{2}+\sum_{n=1}^{\infty}[c_n(r)\sin(n\vartheta)+h_n(r)\cos(n\vartheta)]. \tag{27}$$

By substituting Eqs. (26) and (27) in Eq. (11), one obtains

$$\frac{1}{2}\left(\frac{d^2c_0}{dr^2}+\frac{1}{r}\frac{dc_0}{dr}\right)+\frac{\lambda}{4}+\sum_{n=1}^{\infty}\left[\frac{d^2c_n}{dr^2}+\frac{1}{r}\frac{dc_n}{dr}-\frac{n^2}{r^2}c_n+\frac{1}{4}\frac{Gr}{Re}r^na_n(1)\right]\sin(n\vartheta)+\sum_{n=1}^{\infty}\left[\frac{d^2h_n}{dr^2}+\frac{1}{r}\frac{dh_n}{dr}-\frac{n^2}{r^2}h_n+\frac{1}{4}\frac{Gr}{Re}r^nb_n(1)\right]\cos(n\vartheta)=0. \tag{28}$$

Moreover, Eqs. (13) and (27) yield

$$u(1,\vartheta)=\frac{c_0(1)}{2}+\sum_{n=1}^{\infty}[c_n(1)\sin(n\vartheta)+h_n(1)\cos(n\vartheta)]=0. \tag{29}$$

By integrating Eqs. (28) and (29) with respect to ϑ in the range $[0,2\pi]$, one obtains

$$\frac{d^2c_0}{dr^2}+\frac{1}{r}\frac{dc_0}{dr}+\frac{\lambda}{2}=0 \tag{30}$$

and

$$c_0(1) = 0. \tag{31}$$

The solution of Eqs. (30) and (31) which is finite for $r = 0$ is given by

$$c_0(r) = \frac{\lambda}{8}(1 - r^2). \tag{32}$$

The value of the parameter λ is determined by Eq. (15). Indeed, Eqs. (15), (27) and (32) yield

$$\int_0^{2\pi} \mathrm{d}\vartheta \int_0^1 \mathrm{d}r\, r \left\{ \frac{\lambda}{16}(1 - r^2) + \sum_{n=1}^{\infty} [c_n(r)\sin(n\vartheta) + h_n(r)\cos(n\vartheta)] \right\} = \pi, \tag{33}$$

so that one obtains

$$\lambda = 32. \tag{34}$$

If one multiplies Eqs. (28) and (29) by $\sin(m\vartheta)$, where m is an arbitrary positive integer, and then integrates with respect to ϑ in the range $[0, 2\pi]$, one obtains

$$\frac{\mathrm{d}^2 c_n}{\mathrm{d}r^2} + \frac{1}{r}\frac{\mathrm{d}c_n}{\mathrm{d}r} - \frac{n^2}{r^2}c_n + \frac{1}{4}\frac{Gr}{Re}a_n(1)r^n = 0 \tag{35}$$

and

$$c_n(1) = 0. \tag{36}$$

The solution of Eqs. (35) and (36) which is finite for $r = 0$ is

$$c_n(r) = \frac{Gr}{Re}\frac{a_n(1)}{16(n+1)}(1 - r^2)r^n. \tag{37}$$

Similarly, by multiplying Eqs. (28) and (29) by $\cos(m\vartheta)$ and then integrating with respect to ϑ in the range $[0, 2\pi]$, one obtains

$$\frac{\mathrm{d}^2 h_n}{\mathrm{d}r^2} + \frac{1}{r}\frac{\mathrm{d}h_n}{\mathrm{d}r} - \frac{n^2}{r^2}h_n + \frac{1}{4}\frac{Gr}{Re}b_n(1)r^n = 0 \tag{38}$$

and

$$h_n(1) = 0. \tag{39}$$

The solution of Eqs. (38) and (39) which is finite for $r = 0$ is

$$h_n(r) = \frac{Gr}{Re}\frac{b_n(1)}{16(n+1)}(1 - r^2)r^n. \tag{40}$$

On account of Eqs. (27), (32), (34), (37) and (40), the dimensionless velocity distribution is given by

$$u(r, \vartheta) = u^{(1)}(r) + \frac{Gr}{Re}u^{(2)}(r, \vartheta), \tag{41}$$

where

$$u^{(1)}(r) = 2(1 - r^2), \tag{42}$$

$$u^{(2)}(r, \vartheta) = \frac{1}{16}(1 - r^2)\sum_{n=1}^{\infty}\frac{r^n}{n+1}[a_n(1)\sin(n\vartheta) + b_n(1)\cos(n\vartheta)]. \tag{43}$$

On account of Eqs. (41)–(43), in the limit $Gr/Re \to 0$, $u(r, \vartheta)$ tends to $u^{(1)}(r)$, *i.e.* the dimensionless velocity distribution coincides with the Poiseuille dimensionless velocity profile. Indeed, the limit $Gr/Re \to 0$ represents the forced convection regime. Moreover, if one defines a modified dimensionless velocity through the expression

$$u^*(r, \vartheta) = \frac{Re}{Gr}u(r, \vartheta) = \frac{\nu}{4g\beta\Delta T R_0^2}U(R, \vartheta), \tag{44}$$

$u^{(2)}(r, \vartheta)$ coincides with the limit of $u^*(r, \vartheta)$ for $Gr/Re \to \infty$. This limit corresponds to the case of free convection (purely buoyancy-driven flow).

The Fanning friction factor f is defined as

$$f = \frac{2\tau_w}{\varrho_0 U_0^2}, \tag{45}$$

where the average wall shear stress τ_w is given by

$$\tau_w = -\frac{\mu}{2\pi}\int_0^{2\pi}\left.\frac{\partial U}{\partial R}\right|_{R=R_0}\mathrm{d}\vartheta. \tag{46}$$

By substituting Eq. (46) in Eq. (45), one obtains

$$f = -\frac{\nu}{\pi U_0^2}\int_0^{2\pi}\left.\frac{\partial U}{\partial R}\right|_{R=R_0}\mathrm{d}\vartheta = -\frac{2}{\pi}\frac{1}{Re}\int_0^{2\pi}\left.\frac{\partial u}{\partial r}\right|_{r=1}\mathrm{d}\vartheta. \tag{47}$$

If one integrates both sides of Eq. (11) with respect to r and ϑ in the whole unit circle $r < 1$, one is led to the expression:

$$\lambda\pi + 4\int_0^{2\pi}\left.\frac{\partial u}{\partial r}\right|_{r=1}\mathrm{d}\vartheta = 0. \tag{48}$$

Eqs. (47) and (48) yield the relation

$$f\,Re = \frac{\lambda}{2}. \tag{49}$$

The assumption that the average wall heat flux is zero implies that the average Nusselt number is zero as well. On the other hand, the local Nusselt number Nu_ϑ is given by

$$Nu_\vartheta = \frac{2R_0 h_\vartheta}{k} = \frac{2R_0 q_{w_\vartheta}}{k[T(R_0, \vartheta) - T_b]}, \tag{50}$$

where h_ϑ is the local convection coefficient, k is the thermal conductivity of the fluid, q_{w_ϑ} is the local inward wall heat flux per unit area, and T_b is the bulk temperature. By employing Eq. (8), T_b can be expressed as

$$T_b = \frac{1}{\pi R_0^2 U_0}\int_0^{2\pi}\mathrm{d}\vartheta\int_0^{R_0}\mathrm{d}R\,RUT = \frac{\Delta T}{\pi}\int_0^{2\pi}\mathrm{d}\vartheta\int_0^1\mathrm{d}r\,rut + T_0. \tag{51}$$

If one defines the dimensionless bulk temperature,

$$t_{\mathrm{b}} = \frac{T_{\mathrm{b}} - T_0}{\Delta T} = \frac{1}{\pi}\int_0^{2\pi} \mathrm{d}\vartheta \int_0^1 \mathrm{d}r\, r u t \tag{52}$$

and employs the dimensionless quantities given by Eq. (8), one can write the local Nusselt number as

$$Nu_\vartheta = \frac{2}{t(1,\vartheta) - t_{\mathrm{b}}} \left.\frac{\partial t}{\partial r}\right|_{r=1}. \tag{53}$$

On account of Eqs. (41) and (52), the dimensionless bulk temperature t_{b} can be expressed as

$$t_{\mathrm{b}} = t_{\mathrm{b}}^{(1)} + \frac{Gr}{Re} t_{\mathrm{b}}^{(2)}, \tag{54}$$

where

$$t_{\mathrm{b}}^{(1)} = \frac{1}{\pi}\int_0^{2\pi} \mathrm{d}\vartheta \int_0^1 \mathrm{d}r\, r u^{(1)}(r) t(r,\vartheta), \tag{55}$$

$$t_{\mathrm{b}}^{(2)} = \frac{1}{\pi}\int_0^{2\pi} \mathrm{d}\vartheta \int_0^1 \mathrm{d}r\, r u^{(2)}(r,\vartheta) t(r,\vartheta). \tag{56}$$

As a consequence of Eqs. (53) and (54), the inverse of the local Nusselt number is a linear function of Gr/Re, namely

$$\frac{1}{Nu_\vartheta} = A(\vartheta) - \frac{Gr}{Re} B(\vartheta), \tag{57}$$

where

$$A(\vartheta) = \frac{1}{2}\left[t(1,\vartheta) - t_{\mathrm{b}}^{(1)}\right]\left(\left.\frac{\partial t}{\partial r}\right|_{r=1}\right)^{-1}, \tag{58}$$

$$B(\vartheta) = \frac{1}{2} t_{\mathrm{b}}^{(2)}\left(\left.\frac{\partial t}{\partial r}\right|_{r=1}\right)^{-1}. \tag{59}$$

To summarize, the solution obtained in this section shows that the buoyancy forces do not affect either the dimensionless temperature distribution, or the dimensionless pressure drop λ, or the Fanning friction factor f. On the contrary, the dimensionless velocity distribution and the local Nusselt number depend on Gr/Re.

4. Sinusoidal wall temperature distribution

In this section, the general solution obtained above is applied to the case of a duct with a sinusoidal wall temperature distribution having a period $2\pi/q$, where q is an arbitrary positive integer.

The thermal boundary condition can be expressed as

$$T(R_0,\vartheta,X) = \sin(q\vartheta)\Delta T + T_{\mathrm{w}}, \tag{60}$$

where the constant T_{w} is the mean wall temperature. On account of Eq. (3), it is easily proved that the boundary condition expressed by Eq. (60) yields $\partial T/\partial X = 0$. Indeed, if one differentiates both sides of Eq. (3) with respect to X, one obtains

$$\frac{\partial T}{\partial X} = \frac{\mathrm{d}T_0}{\mathrm{d}X} + \frac{1}{\varrho_0 g\beta}\frac{\mathrm{d}^2 P}{\mathrm{d}X^2}. \tag{61}$$

Obviously, the right hand side of Eq. (61) does not depend on R and ϑ, so that the value of $\partial T/\partial X$ at every inner position coincides with the value at the wall. Since the wall temperature is independent of X, one concludes that $\partial T/\partial X = 0$ for every value of R and ϑ.

By introducing the dimensionless quantity

$$\eta = \frac{T_{\mathrm{w}} - T_0}{\Delta T} \tag{62}$$

and employing Eq. (8), one can write Eq. (60) in the dimensionless form

$$t(1,\vartheta) = \sin(q\vartheta) + \eta. \tag{63}$$

Eqs. (26) and (63) yield

$$\eta = 0, \quad a_n(1) = \delta_{q,n}, \quad b_n(1) = 0, \tag{64}$$

where $\delta_{q,n}$ is Kronecker's delta.

On account of Eqs. (26) and (64), the dimensionless temperature distribution is

$$t(r,\vartheta) = r^q \sin(q\vartheta), \tag{65}$$

whereas, as a consequence of Eqs. (43) and (64), the buoyancy-induced dimensionless velocity term $u^{(2)}$ is given by

$$u^{(2)}(r,\vartheta) = \frac{1}{16}(1-r^2)\frac{r^q}{q+1}\sin(q\vartheta). \tag{66}$$

In Fig. 2, the function $u^{(2)}(r,\vartheta)$ is plotted versus ϑ for $r = 0.5$ and for three values of q. The figure shows that $u^{(2)}(r,\vartheta)$ is positive if and only if $2m\pi/q < \vartheta < (2m+1)\pi/q$, where m is any non-negative integer. Therefore, Eq. (41) implies that, if $Gr/Re > 0$, the dimensionless velocity $u(r,\vartheta)$ is greater than $u^{(1)}(r)$ for $2m\pi/q < \vartheta < (2m+1)\pi/q$ and lower elsewhere. Moreover, Fig. 2 shows that the effect of buoyancy on the dimensionless velocity distribution becomes less important as q increases.

It can be easily verified that, due to the special symmetry of the thermal boundary condition,

$$t_{\mathrm{b}}^{(1)} = 0 \tag{67}$$

for every value of the parameter q. On the other hand, the term $t_{\mathrm{b}}^{(2)}$ is given by

$$t_{\mathrm{b}}^{(2)} = \frac{1}{32(q+1)^2(q+2)}. \tag{68}$$

It is easily shown that, for every q, there exists a positive real number $(Gr/Re)_{\mathrm{FR}}$ such that flow reversal occurs for upward flow when $Gr/Re > (Gr/Re)_{\mathrm{FR}}$ and for down-

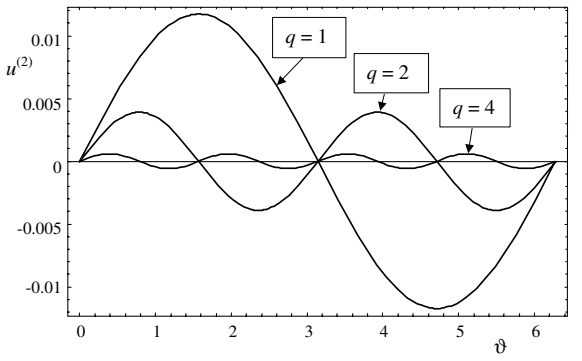

Fig. 2. Buoyancy-induced dimensionless velocity term $u^{(2)}$ as a function of ϑ, for $r = 0.5$ and for three values of q.

ward flow when $Gr/Re < -(Gr/Re)_{FR}$. Indeed, for $Gr/Re = (Gr/Re)_{FR}$, the first derivative of $u(r,\vartheta)$, evaluated for $r = 1$ and $\vartheta = 3\pi/(2q)$, vanishes. One obtains

$$\left(\frac{Gr}{Re}\right)_{FR} = -\left.\frac{du^{(1)}}{dr}\right|_{r=1}\left[\left.\frac{\partial u^{(2)}}{\partial r}\right|_{r=1,\vartheta=3\pi/(2q)}\right]^{-1} = 32(q+1). \tag{69}$$

In Figs. 3–5 the dimensionless velocity distribution $u(r,\vartheta)$ is plotted for $q = 1$ and $Gr/Re = 200$, $q = 2$ and $Gr/Re = 400$, $q = 4$ and $Gr/Re = 600$, respectively. The figures show that, for these values of q and Gr/Re, strong deformations of the Poiseuille dimensionless-velocity distribution occur. Namely, values of u higher than 2 can take place in the warmer parts of the tube, while negative values of u are present close to the cooler parts of the wall (flow reversal).

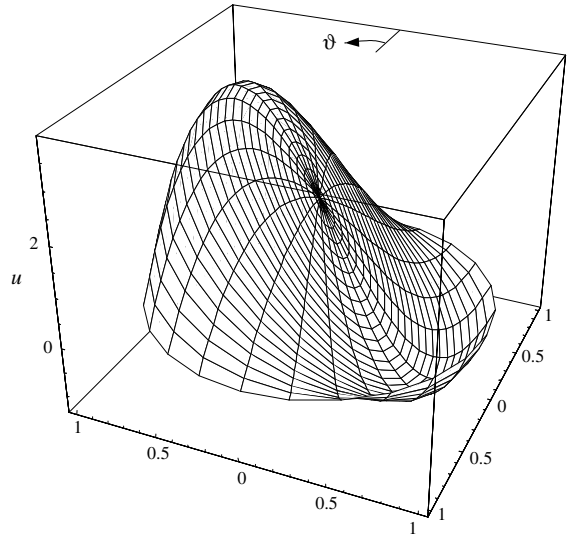

Fig. 3. Dimensionless velocity distribution for $q = 1$ and $Gr/Re = 200$.

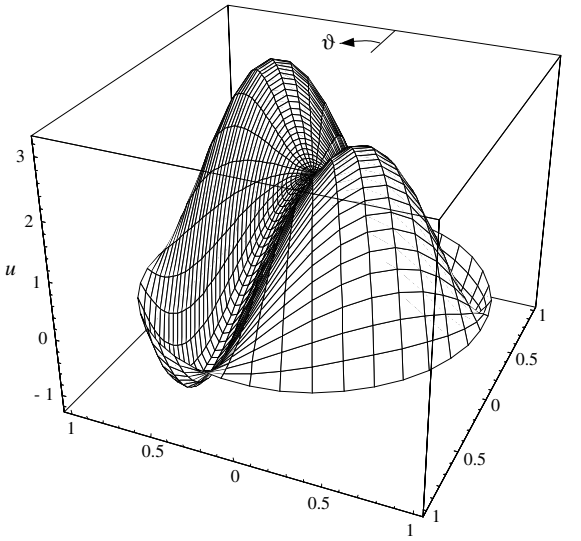

Fig. 4. Dimensionless velocity distribution for $q = 2$ and $Gr/Re = 400$.

Eqs. (53), (65), (67) and (68) lead to the following expression of the local Nusselt number

$$Nu_\vartheta = \frac{64q(q+1)^2(q+2)\sin(q\vartheta)}{32(q+1)^2(q+2)\sin(q\vartheta) - Gr/Re}. \tag{70}$$

Therefore, singularities of Nu_ϑ may occur if Gr/Re is such that

$$-32(q+1)^2(q+2) < \frac{Gr}{Re} < 32(q+1)^2(q+2). \tag{71}$$

These singularities occur for

$$\vartheta = \frac{1}{q}\arcsin\left[\frac{Gr/Re}{32(q+1)^2(q+2)}\right] + \frac{2m\pi}{q} \tag{72}$$

and for

$$\vartheta = \frac{\pi}{q} - \frac{1}{q}\arcsin\left[\frac{Gr/Re}{32(q+1)^2(q+2)}\right] + \frac{2m\pi}{q}, \tag{73}$$

where m is any non-negative integer.

5. External convection with two environments

As a second example, let us consider a duct subjected to an external convection heat transfer with two environments having different reference temperatures, T_1 and T_2. Moreover, let us assume that the external convection coefficient h_e is uniform on the whole duct wall and that $T_1 > T_2$. This thermal boundary condition is represented in Fig. 6 and can be expressed as

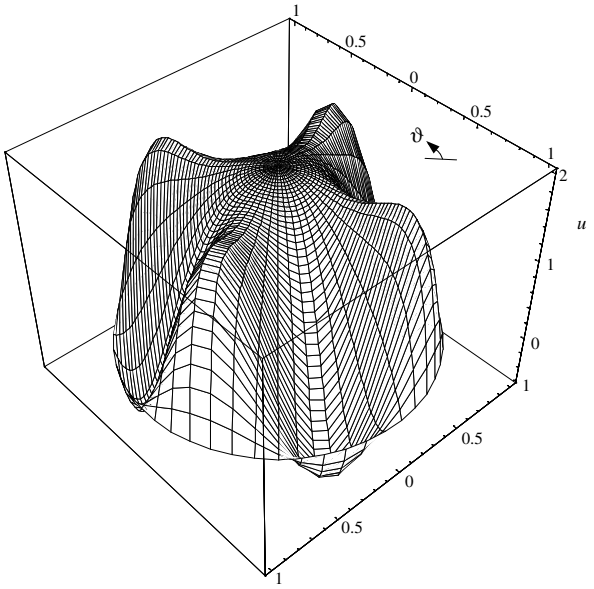

Fig. 5. Dimensionless velocity distribution for $q = 4$ and $Gr/Re = 600$.

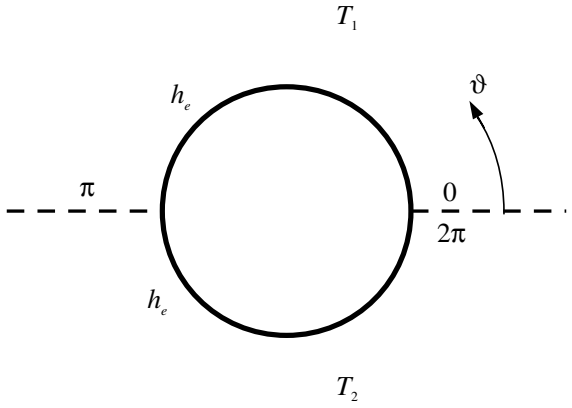

Fig. 6. External convection heat transfer.

$$-\left.\frac{\partial T}{\partial R}\right|_{R=R_0} = \frac{h_e}{k}[T(R_0,\vartheta,X) - F(\vartheta)\Delta T - T_m], \tag{74}$$

where

$$\begin{aligned} &F(\vartheta) = +1, \quad \text{for } 0 < \vartheta < \pi, \\ &F(\vartheta) = -1, \quad \text{for } \pi < \vartheta < 2\pi \end{aligned} \tag{75}$$

and

$$\Delta T = \frac{T_1 - T_2}{2}, \quad T_m = \frac{T_1 + T_2}{2}. \tag{76}$$

As it is proved in Appendix A, the boundary condition expressed by Eqs. (74)–(76) yields $\partial T/\partial X = 0$. Then, Eq. (74) can be rewritten in the dimensionless form

$$-\left.\frac{\partial t}{\partial r}\right|_{r=1} = Bi[t(1,\vartheta) - F(\vartheta)], \tag{77}$$

where the Biot number Bi is given by

$$Bi = \frac{h_e R_0}{k}. \tag{78}$$

On account of Eq. (77), the limit $Bi \to \infty$ corresponds to $t(1,\vartheta) \to F(\vartheta)$. In this limit, which is attained when h_e tends to infinity, one recovers the case of a piecewise uniform wall temperature.

On account of Eqs. (26) and (77), by employing the orthogonality of sine and cosine functions, one obtains

$$\begin{aligned} &a_{2n}(1) = 0, \\ &a_{2n-1}(1) = \frac{4Bi}{\pi(2n-1)(2n-1+Bi)}, \quad b_n(1) = 0 \end{aligned} \tag{79}$$

for every positive integer n.

To summarize, the dimensionless temperature $t(r,\vartheta)$ and the dimensionless velocity term $u^{(2)}(r,\vartheta)$ can be expressed as

$$t(r,\vartheta) = \frac{4Bi}{\pi}\sum_{n=1}^{\infty}\frac{r^{2n-1}}{(2n-1)(2n-1+Bi)}\sin[(2n-1)\vartheta], \tag{80}$$

$$u^{(2)}(r,\vartheta) = \frac{Bi(1-r^2)}{8\pi}\sum_{n=1}^{\infty}\frac{r^{2n-1}}{n(2n-1)(2n-1+Bi)} \times \sin[(2n-1)\vartheta]. \tag{81}$$

In Fig. 7, the dimensionless temperature distribution $t(r,\vartheta)$, evaluated for $r = 1$ and for some values of Bi, is

plotted. This figure shows that, for high values of Bi, the dimensionless wall temperature becomes quite similar to a piecewise uniform function of ϑ. On the other hand, in Fig. 8, plots of $t(r,\vartheta)$ on the vertical plane defined by the relation $\vartheta = \pi/2,\ 3\pi/2$ are reported for some values of Bi.

In Fig. 9, the dimensionless velocity term $u^{(2)}(r,\vartheta)$ is plotted as a function of ϑ, for $r = 0.5$ and for some values of Bi. In Fig. 10, plots of $u^{(2)}(r,\vartheta)$ on the vertical plane defined by the relation $\vartheta = \pi/2,\ 3\pi/2$ are represented for some values of Bi. Figs. 9 and 10 show that the effect of buoyancy on the velocity distribution becomes more important when the Biot number increases.

As in the case of a sinusoidal wall temperature, the symmetry of the thermal boundary condition implies that

$$t_{\mathrm{b}}^{(1)} = 0, \tag{82}$$

for every value of the parameter Bi. On the other hand, from Eqs. (56), (80) and (81) one obtains

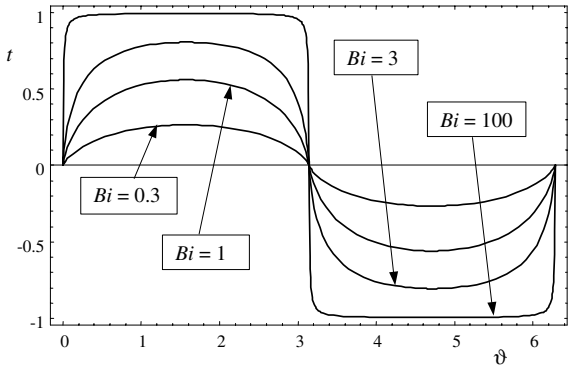

Fig. 7. Dimensionless wall temperature distribution as a function of ϑ, for some values of Bi.

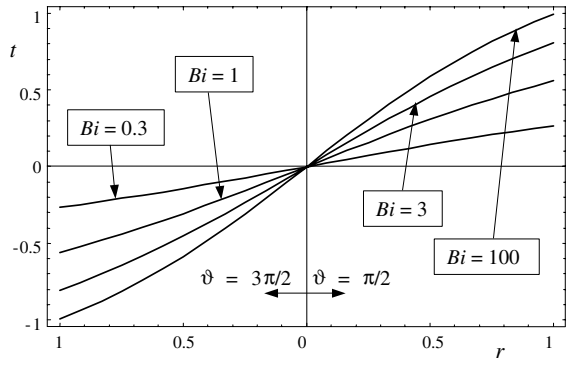

Fig. 8. Dimensionless temperature distribution as a function of r, for $\vartheta = \pi/2,\ 3\pi/2$.

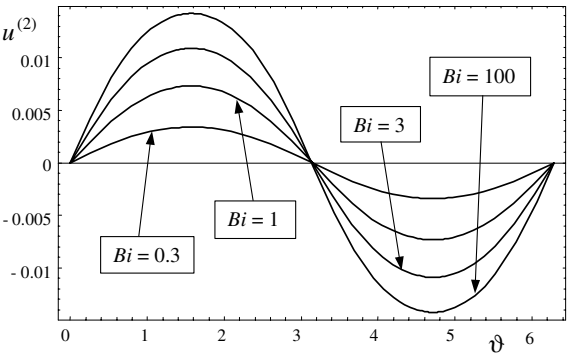

Fig. 9. Buoyancy-induced dimensionless velocity term $u^{(2)}$ as a function of ϑ, for $r = 0.5$.

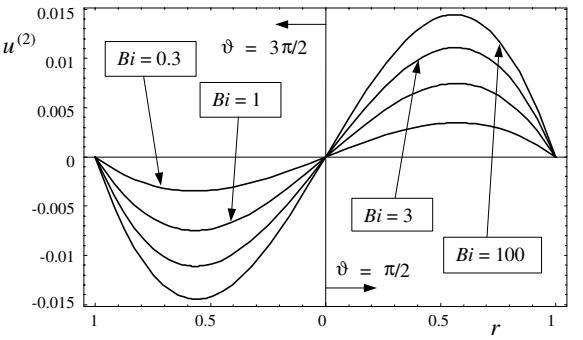

Fig. 10. Buoyancy-induced dimensionless velocity term $u^{(2)}$ as a function of r, for $\vartheta = \pi/2,\ 3\pi/2$.

$$t_{\mathrm{b}}^{(2)} = \frac{Bi^2}{8\pi^2}\sum_{n=1}^{\infty}\frac{1}{n^2(2n-1)^2(2n-1+Bi)^2(2n+1)}. \tag{83}$$

The conditions for the onset of flow reversal can be obtained by a method similar to that employed in the case of a sinusoidal wall temperature distribution, discussed in the preceding section. For every Bi, there exists a positive real number $(Gr/Re)_{\mathrm{FR}}$ such that flow reversal occurs for $Gr/Re > (Gr/Re)_{\mathrm{FR}}$ and for $Gr/Re < -(Gr/Re)_{\mathrm{FR}}$. Indeed, for $Gr/Re = (Gr/Re)_{\mathrm{FR}}$, the first derivative of $u(r,\vartheta)$, evaluated for $r = 1$ and $\vartheta = 3\pi/2$, vanishes. One obtains

$$\left(\frac{Gr}{Re}\right)_{\mathrm{FR}} = -\left.\frac{\mathrm{d}u^{(1)}}{\mathrm{d}r}\right|_{r=1}\left(\left.\frac{\partial u^{(2)}}{\partial r}\right|_{r=1,\vartheta=3\pi/2}\right)^{-1}$$
$$= \frac{16\pi}{Bi}\left[\sum_{n=1}^{\infty}\frac{(-1)^{n+1}}{n(2n-1)(2n-1+Bi)}\right]^{-1}. \tag{84}$$

In Table 1, the values of $t_{\mathrm{b}}^{(2)}$ and of $(Gr/Re)_{\mathrm{FR}}$ are reported for a wide range of Biot numbers. This table shows that $t_{\mathrm{b}}^{(2)}$ is an increasing function of Bi, while $(Gr/Re)_{\mathrm{FR}}$ is a decreasing function of Bi.

Table 1
Values of $t_b^{(2)}$, $(Gr/Re)_{FR}$ and $(Gr/Re)_{sing}$

Bi	$t_b^{(2)}$	$(Gr/Re)_{FR}$	$(Gr/Re)_{sing}$
0.01	4.14666×10^{-7}	5.32166×10^{3}	2.78304×10^{4}
0.02	1.62634×10^{-6}	2.68799×10^{3}	1.40446×10^{4}
0.03	3.58866×10^{-6}	1.81011×10^{3}	9.44922×10^{3}
0.04	6.25790×10^{-6}	1.37118×10^{3}	7.15149×10^{3}
0.05	9.59286×10^{-6}	1.10782×10^{3}	5.77282×10^{3}
0.06	1.35547×10^{-5}	9.32249×10^{2}	4.85367×10^{3}
0.07	1.81066×10^{-5}	8.06846×10^{2}	4.19710×10^{3}
0.08	2.32142×10^{-5}	7.12797×10^{2}	3.70466×10^{3}
0.09	2.88446×10^{-5}	6.39649×10^{2}	3.32162×10^{3}
0.1	3.49670×10^{-5}	5.81133×10^{2}	3.01517×10^{3}
0.2	1.17558×10^{-4}	3.17863×10^{2}	1.63565×10^{3}
0.3	2.25436×10^{-4}	2.30165×10^{2}	1.17524×10^{3}
0.4	3.45655×10^{-4}	1.86356×10^{2}	9.44644×10^{2}
0.5	4.70592×10^{-4}	1.60101×10^{2}	8.06011×10^{2}
1.0	1.06009×10^{-3}	1.07770×10^{2}	5.27062×10^{2}
2.0	1.88835×10^{-3}	81.9049	3.84868×10^{2}
3.0	2.39365×10^{-3}	73.4337	3.36164×10^{2}
4.0	2.72678×10^{-3}	69.2596	3.11296×10^{2}
5.0	2.96166×10^{-3}	66.7847	2.96134×10^{2}
10.0	3.53510×10^{-3}	61.9309	2.65048×10^{2}
20.0	3.88899×10^{-3}	59.5709	2.48984×10^{2}
50.0	4.12912×10^{-3}	58.1836	2.39130×10^{2}
100.0	4.21455×10^{-3}	57.7267	2.35822×10^{2}

In Figs. 11 and 12, the dimensionless velocity distribution $u(r, \vartheta)$ is represented for $Gr/Re = 300$, respectively for $Bi = 0.3$ and $Bi = 100$. Both figures show that, for these values of Bi and Gr/Re, a considerable discrepancy with respect to the Poiseuille dimensionless-velocity distribution occurs. The deformation of the velocity profile is sharper for $Bi = 100$ (Fig. 12) than for $Bi = 0.3$ (Fig. 11) and the region of flow reversal is wider.

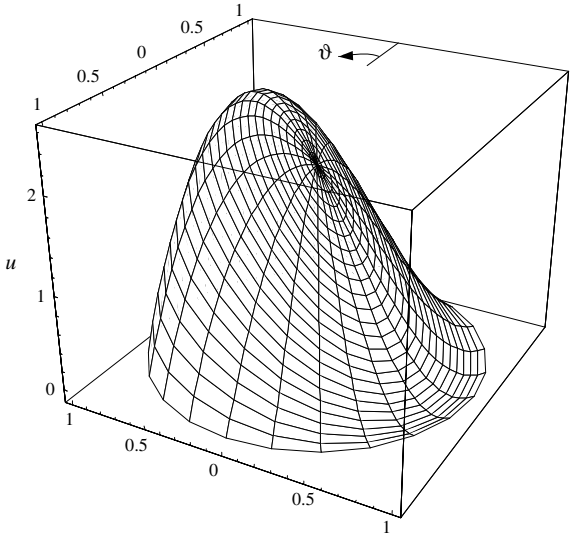

Fig. 11. Dimensionless velocity distribution for $Bi = 0.3$ and $Gr/Re = 300$.

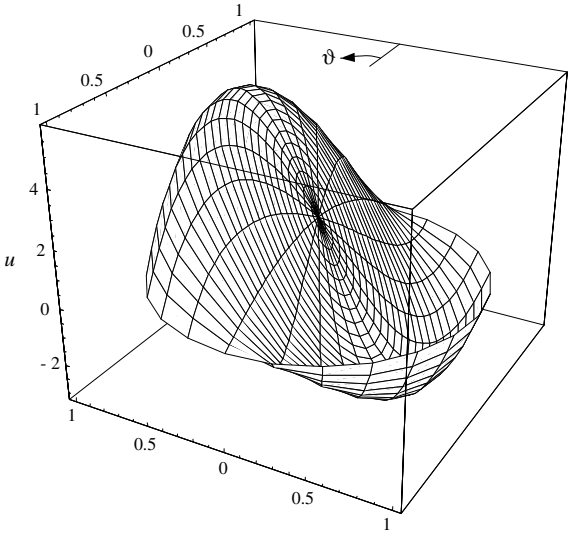

Fig. 12. Dimensionless velocity distribution for $Bi = 100$ and $Gr/Re = 300$.

On account of Eqs. (80), (82) and (83), the functions A and B defined in Section 3 and given by Eqs. (58) and (59), have the following expressions:

$$A(\vartheta)=\frac{1}{2}\left\{\sum_{n=1}^{\infty}\frac{\sin[(2n-1)\vartheta]}{(2n-1)(2n-1+Bi)}\right\}\times\left\{\sum_{n=1}^{\infty}\frac{\sin[(2n-1)\vartheta]}{(2n-1+Bi)}\right\}^{-1}, \tag{85}$$

$$B(\vartheta)=\frac{Bi}{64\pi}\left[\sum_{n=1}^{\infty}\frac{1}{n^2(2n-1)^2(2n-1+Bi)^2(2n+1)}\right]\times\left\{\sum_{n=1}^{\infty}\frac{\sin[(2n-1)\vartheta]}{(2n-1+Bi)}\right\}^{-1}. \tag{86}$$

It can be easily verified that, for any given value of Bi, $A(\vartheta)$ and $B(\vartheta)$ satisfy the following conditions:

$$A(\vartheta)=A(\pi-\vartheta),\quad A(\vartheta)=A(2\pi-\vartheta), \tag{87}$$

$$B(\vartheta)=B(\pi-\vartheta),\quad B(\vartheta)=-B(2\pi-\vartheta). \tag{88}$$

On account of Eqs. (57), (87) and (88), Nu_ϑ is a symmetric function of ϑ with respect to $\vartheta=\pi/2$. Moreover, for $Gr/Re=0$ (forced convection), Nu_ϑ is also a symmetric function of ϑ with respect to $\vartheta=\pi$. The latter symmetry does not occur for mixed convection ($Gr/Re\neq 0$). In Figs. 13 and 14, plots of A and B as functions of ϑ are shown in the range $[0,\pi/2]$, for three different values of Bi. Both $A(\vartheta)$ and $B(\vartheta)$ are increasing functions of ϑ in the range $[0,\pi/2]$. While $A(0)=0$, the value of $B(0)$ depends on the Biot number.

Eq. (57) reveals that the local Nusselt number is singular when $A(\vartheta)/B(\vartheta)=Gr/Re$. In Fig. 15, the ratio A/B as a function of ϑ is shown in the range $[0,\pi/2]$, for three different values of Bi. In this range, the ratio A/B is an increasing function of ϑ and has its maximum for $\vartheta=\pi/2$. Therefore, by employing Eqs. (57), (87) and (88), one can infer that Nu_ϑ presents singularities only if, for a given Bi, the absolute value of Gr/Re is lower than $A(\pi/2)/B(\pi/2)$. In the following, the ratio $A(\pi/2)/B(\pi/2)$ will be denoted as $(Gr/Re)_{\text{sing}}$. A qualitative representation of the singularities of Nu_ϑ can be found in Fig. 16. On account of Eqs. (87) and (88), it is easily shown that $A(\vartheta)/B(\vartheta)$ is symmetric with respect to $\vartheta=\pi/2$ and antisymmetric with respect to $\vartheta=\pi$. Therefore, for a given value of Bi and for a positive value of Gr/Re such that $Gr/Re<(Gr/Re)_{\text{sing}}$, Nu_ϑ presents two singularities: one in $\vartheta=\vartheta_{\text{sing}}(\vartheta_{\text{sing}}<\pi/2)$ and the other in $\vartheta=\pi-\vartheta_{\text{sing}}$. The value of ϑ_{sing} can be determined by finding the roots of the following equation:

$$\frac{A(\vartheta)}{B(\vartheta)}=\frac{Gr}{Re}. \tag{89}$$

Obviously, for a given value of Bi and for a negative value of Gr/Re such that $Gr/Re>-(Gr/Re)_{\text{sing}}$, Nu_ϑ presents two singularities: one in $\vartheta=\vartheta_{\text{sing}}(\pi<\vartheta_{\text{sing}}<3\pi/2)$ and the other in $\vartheta=2\pi-\vartheta_{\text{sing}}$. Also in this case, the value of ϑ_{sing} can be determined by finding the roots of Eq. (89). In the last column of Table 1, values of $(Gr/Re)_{\text{sing}}$ are reported for several Biot numbers. This table shows that $(Gr/Re)_{\text{sing}}$ is a decreasing function of Bi.

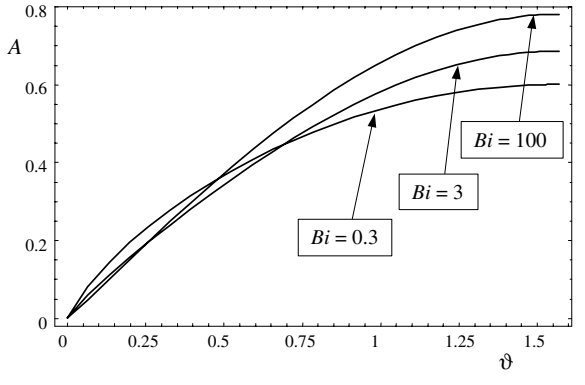

Fig. 13. Plots of A versus ϑ, for different values of Bi.

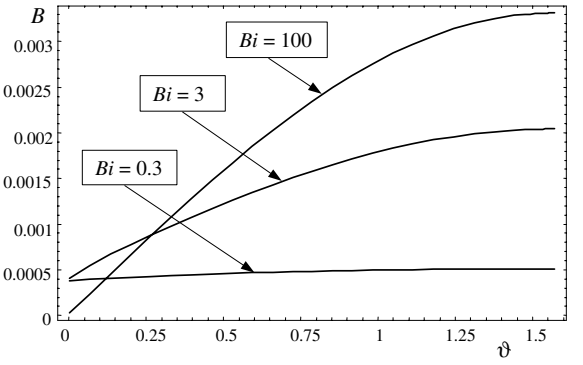

Fig. 14. Plots of B versus ϑ, for different values of Bi.

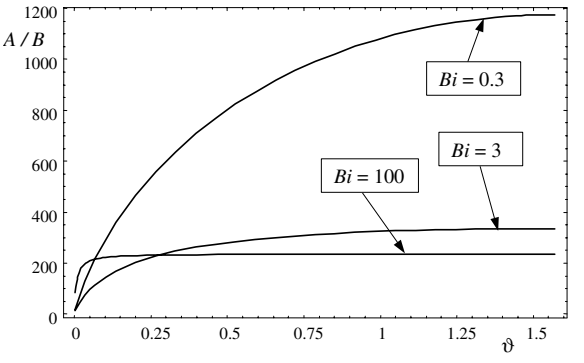

Fig. 15. Plots of the ratio A/B versus ϑ, for different values of Bi.

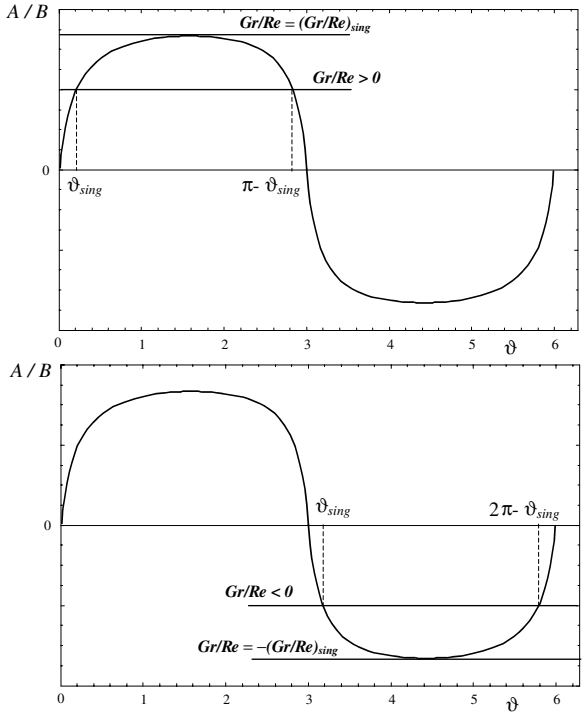

Fig. 16. Existence of singularities of Nu_ϑ, for a given value of Bi.

6. Conclusions

The combined forced and free convection in a vertical circular duct has been analyzed by employing Fourier series expansions of the dimensionless temperature and velocity fields. Non-axisymmetric thermal boundary conditions have been considered, such that the fluid temperature is independent of the axial coordinate. Two special cases have been investigated: a duct subjected to a sinusoidal wall temperature distribution; a duct subjected to external convection with two environments having different reference temperatures. The most important results obtained are the following.

- For an arbitrary thermal boundary condition which does not yield a net fluid heating, buoyancy forces do not affect the dimensionless temperature distribution, the dimensionless pressure drop parameter and the Fanning friction factor. Thus, these quantities are independent of the ratio Gr/Re. On the other hand, the inverse of the local Nusselt number is a linear function of Gr/Re.
- In the first example (sinusoidal wall temperature distribution), the dimensionless velocity distribution depends both on Gr/Re and on the angular frequency q. In the second example (external convection with two environments), the dimensionless velocity distribution depends both on Gr/Re and on the Biot number Bi. In both examples, it has been shown that, either for every q (first example) or for every Bi (second example), there exists a positive real number $(Gr/Re)_{\mathrm{FR}}$ such that flow reversal occurs for upward flow when $Gr/Re > (Gr/Re)_{\mathrm{FR}}$ and for downward flow when $Gr/Re < -(Gr/Re)_{\mathrm{FR}}$. The threshold value, $(Gr/Re)_{\mathrm{FR}}$, has been determined as a function of q in the first example and of Bi in the second example. In both examples, the local Nusselt number presents singularities for sufficiently small values of $|Gr/Re|$.

Appendix A

In the case of a steady parallel flow, the energy balance equation can be written as

$$U\frac{\partial T}{\partial X} = \alpha\nabla^2 T, \tag{A.1}$$

where α is the fluid thermal diffusivity. If the duct is subjected to external convection with an environment having a reference temperature T_f which depends on the angular coordinate ϑ, the thermal boundary condition can be written as

$$-k\left.\frac{\partial T}{\partial R}\right|_{R=R_0} = h_{\mathrm{e}}[T(R_0,\vartheta,X) - T_f(\vartheta)], \tag{A.2}$$

where the external convection coefficient h_e is assumed to be uniform on the whole duct wall.

It will be shown that the thermal boundary condition defined by (A.2) yields $\partial T/\partial X = 0$, provided that the fully developed region is considered.

The mean value of an arbitrary quantity G over a duct section is defined as

$$\langle G\rangle = \frac{1}{\pi R_0^2}\int_S G\,\mathrm{d}S = \frac{1}{\pi R_0^2}\int_0^{2\pi}\mathrm{d}\vartheta\int_0^{R_0}\mathrm{d}R\,RG, \tag{A.3}$$

where S is the duct section. Since the mean value of the fluid velocity U is given by

$$\langle U\rangle = U_0 \tag{A.4}$$

and since $\partial T/\partial X$ is uniform on the duct section, as shown by Eq. (61), the mean value of the left hand side of Eq. (A.1) can be written as

$$\left\langle U\,\frac{\partial T}{\partial X}\right\rangle = U_0\,\frac{\partial T}{\partial X}. \tag{A.5}$$

The mean value of the right hand side of Eq. (A.1) is given by

$$\begin{aligned}\langle\alpha\nabla^2 T\rangle = \alpha\langle\nabla^2 T\rangle &= \frac{\alpha}{\pi R_0^2}\int_S \nabla\cdot\nabla T\,\mathrm{d}S\\ &= \frac{\alpha}{\pi R_0^2}\int_{\partial S}\nabla T\cdot\mathbf{R}\,\mathrm{d}l\\ &= \frac{\alpha}{\pi R_0^2}\int_0^{2\pi}\left.\frac{\partial T}{\partial R}\right|_{R=R_0} R_0\,\mathrm{d}\vartheta\\ &= \frac{\alpha}{\pi R_0}\int_0^{2\pi}\left.\frac{\partial T}{\partial R}\right|_{R=R_0}\mathrm{d}\vartheta,\end{aligned} \tag{A.6}$$

where ∂S is the boundary of S and $\mathbf{R}$ is the radial unit vector. Moreover, by employing the thermal boundary condition given by Eq. (A.2), one obtains

$$\begin{aligned}\frac{\alpha}{\pi R_0}\int_0^{2\pi}\left.\frac{\partial T}{\partial R}\right|_{R=R_0}\mathrm{d}\vartheta &= -\frac{\alpha h_e}{k\pi R_0}\left[\int_0^{2\pi}T(R_0,\vartheta,X)\,\mathrm{d}\vartheta\right.\\ &\quad\left.-\int_0^{2\pi}T_f(\vartheta)\,\mathrm{d}\vartheta\right]\\ &= -\frac{2\alpha h_e}{kR_0}[T_w - T_m],\end{aligned} \tag{A.7}$$

where T_w is the mean wall temperature and T_m is the mean value of $T_f(\vartheta)$. On account of Eqs. (A.5)–(A.7), the energy balance equation (A.1) yields

$$U_0\,\frac{\partial T}{\partial X} = -\frac{2\alpha h_e}{kR_0}[T_w - T_m]. \tag{A.8}$$

If one differentiates both sides of Eq. (A.8) with respect to X, one obtains

$$U_0\,\frac{\partial^2 T}{\partial X^2} = -\frac{2\alpha h_e}{kR_0}\,\frac{\mathrm{d}T_w}{\mathrm{d}X}. \tag{A.9}$$

Since $\partial T/\partial X$ is uniform on a duct section, the following equality holds:

$$\frac{\mathrm{d}T_w}{\mathrm{d}X} = \frac{\partial T}{\partial X}. \tag{A.10}$$

By substituting Eq. (A.10) in Eq. (A.9), one is led to the differential equation

$$U_0\,\frac{\partial^2 T}{\partial X^2} = -\frac{2\alpha h_e}{kR_0}\,\frac{\partial T}{\partial X}. \tag{A.11}$$

Let us define

$$\frac{\partial T}{\partial X} = H(X), \tag{A.12}$$

so that Eq. (A.11) yields

$$U_0\,\frac{\mathrm{d}H(X)}{\mathrm{d}X} = -\frac{2\alpha h_e}{kR_0}H(X). \tag{A.13}$$

The solution of Eq. (A.13) is given by

$$H(X) = H(X_0)\exp\left[-\frac{2\alpha h_e}{kR_0U_0}(X - X_0)\right], \tag{A.14}$$

where X_0 is an arbitrary axial position. Therefore, Eq. (A.14) implies that $H(X) = \partial T/\partial X$ undergoes an exponential decay in the direction of the mean flow. As a consequence, in the fully developed region, $\partial T/\partial X$ tends to zero.

References

[1] W. Aung, Mixed convection in internal flow, in: Handbook of Single-phase Convective Heat Transfer, vol. 15, John Wiley and Sons, New York, 1987.

[2] J.D. Jackson, M.A. Cotton, B.P. Axcell, Studies of mixed convection in vertical tubes, Int. J. Heat Fluid Flow 10 (1989) 2–15.

[3] B.R. Morton, Laminar convection in uniformly heated vertical pipes, J. Fluid Mech. 8 (1960) 227–240.

[4] W.T. Lawrence, J.C. Chato, Heat transfer effects on the developing laminar flow inside vertical tubes, ASME J. Heat Transfer 88 (1966) 214–222.

[5] B. Zeldin, F.W. Schmidt, Developing flow with combined forced-free convection in an isothermal vertical tube, ASME J. Heat Transfer 94 (1972) 211–223.

[6] D. Choudhury, S.V. Patankar, Combined forced and free laminar convection in the entrance region of an inclined isothermal tube, ASME J. Heat Transfer 110 (1988) 901–909.

[7] A. Moutsoglou, Y.D. Kwon, Laminar mixed convection flow in a vertical tube, J. Thermophys. Heat Transfer 7 (1993) 361–368.

[8] J. Orfi, N. Galanis, C.T. Nguyen, Laminar fully developed incompressible flow with mixed convection in inclined tubes, Int. J. Numer. Meth. Heat Fluid Flow 3 (1993) 341–355.

[9] A. Barletta, Combined forced and free convection with viscous dissipation in a vertical circular duct, Int. J. Heat Mass Transfer 42 (1999) 2243–2253.
[10] A. Barletta, E. Rossi di Schio, Effect of viscous dissipation on mixed convection heat transfer in a vertical tube with uniform wall heat flux, Heat Mass Transfer 38 (2001) 129–140.
[11] W.C. Reynolds, Heat transfer to fully developed laminar flow in a circular tube with arbitrary circumferential heat flux, ASME J. Heat Transfer 82 (1960) 108–112.
[12] D.K. Choi, D.H. Choi, Dual solution for mixed convection in a horizontal tube under circumferentially non-uniform heating, Int. J. Heat Mass Transfer 35 (1992) 2053–2056.
[13] D.K. Choi, D.H. Choi, Developing mixed convection flow in a horizontal tube under circumferentially non-uniform heating, Int. J. Heat Mass Transfer 37 (1994) 1899–1913.
[14] A. Barletta, E. Zanchini, On the choice of the reference temperature for fully-developed mixed convection in a vertical channel, Int. J. Heat Mass Transfer 42 (1999) 3169–3181.